Rev. Roum. Sci. Techn.– Électrotechn. et Énerg.
Vol. **64**, *2*, pp. 157–162, Bucarest, 2019

STUDY ON SLIDING MODE CONTROL OF A SMALL SIZE WIND TURBINE PERMANENT MAGNET SYNCHRONOUS GENERATOR SYSTEM

ZOUBIR BOUDRIES[1], SALAH TAMALOUZT[1]

Key words: Permanent magnet synchronous generator (PMSG), Wind turbine, Pulse width modulation (PWM) rectifier, Sliding mode control (SMC), Dc link voltage.

In this paper, we treat a control strategy of the permanent magnet synchronous generator (PMSG) for a small size wind turbine in isolated site. The direct drive PMSG is connected to the dc link through a PWM rectifier. The dc voltage is kept constant at its reference value using a sliding mode control approach, under wind speed and load variations. To ensure the reaching and sustaining of the sliding mode, the Lyapunov direct method is used. The logic control signals (S_a, S_b, S_c) are calculated by using the space vector modulation (SVM) technique. To alleviate chattering phenomenon, a tangent hyperbolic function is used in the dc voltage loop instead of a conventionally used sign function. The simulation results have been performed using Matlab/Simulink environment, they show good tracking performances as well as robustness against external disturbances.

1. INTRODUCTION

Recently, power generation from wind turbines has grown rapidly due to the high pollution generated in conventional production systems and the high cost of fossil fuels [1]. Although most previous studies in this field have concentrated on the development of utility-scale wind powers, small-sized wind energy conversion system (1–100 kW) are getting a lot of attention and become to be very promising solution in remote places or locations where the grid is unavailable [2, 3]. Two types of generators are used in remote areas power supply; these are induction generators (IGs) and permanent magnet synchronous generators (PMSGs) [4–6]. PMSG is preferred to IG because of its multiple advantages. This machine doesn't require any external source and it is connected to the wind turbine directly without gearbox. Furthermore, PMSGs exhibit several characteristics such as large power to weight ratio, high torque to current ratio, high efficiency, high power factor and robustness, small size compared to conventional geared generator based wind turbine [7, 8].

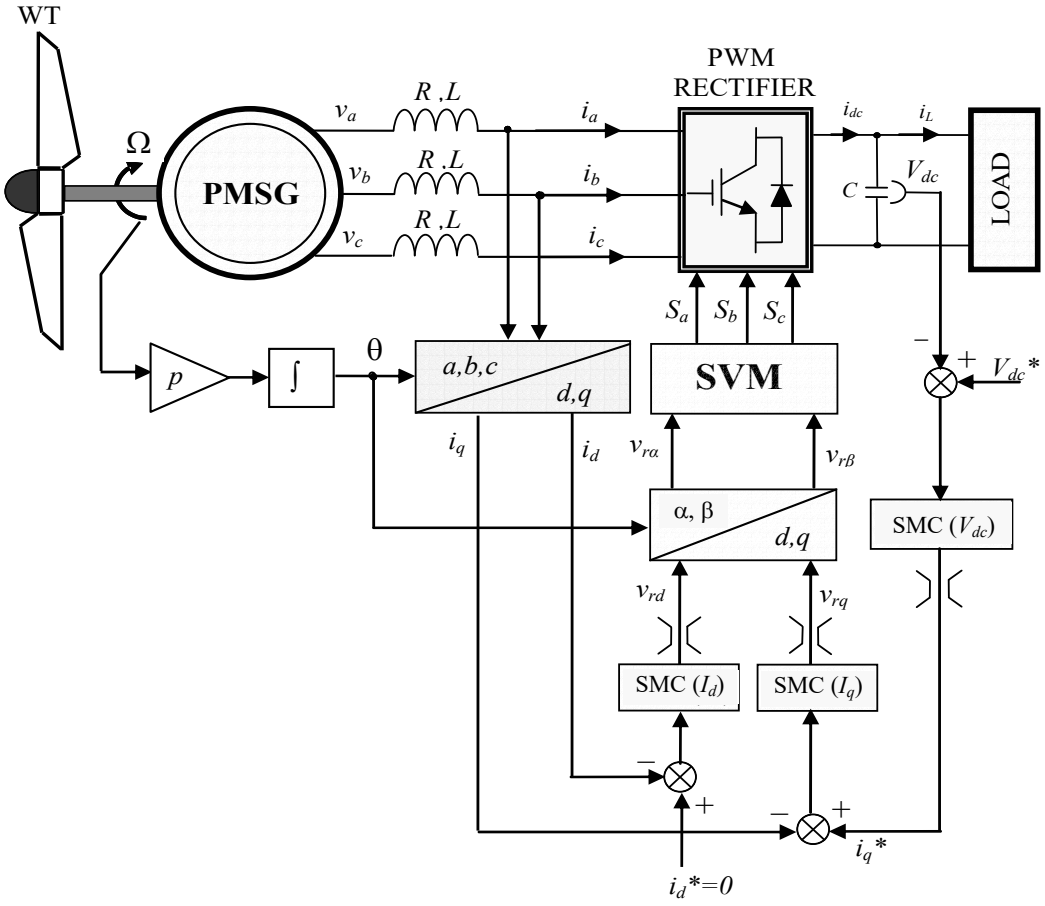

Fig. 1 – The studied system.

[1] Laboratoire de Technologie Industriel et de l'Information (LTII), Faculté de Technologie, Université de Bejaia, Algérie, zboudries@yahoo.fr, tamalouztsalah@yahoo.fr

The power conversion system is necessary to feed loads at desired values of voltage and frequency because the output voltage and frequency of PMSG-wind turbine system depend on wind speed and supply loads. This system should consist converter from ac signals of the generator to dc signals which called PWM rectifier, so that through an inverter (dc/ac converter), the generated power is transmitted to the load. To achieve such a goal, an appropriate control system must be designed; its task is mainly to keep the dc bus voltage constant at its reference value.

Traditionally, the PMSGs control system adopted in a synchronized rotating dq reference frame a decoupled proportional integral (PI) current control scheme [9–13]. The main drawback of this solution is its susceptibility to system parameters changes. In addition, PI controller is a linear regulator, which is inappropriate for wind turbines where the system with both parts electrical and mechanical behavior as a nonlinear system. To overcome this problem, different nonlinear control schemes have been developed [14–16]. Recently, the sliding mode control (SMC) method has been widely used successfully as a nonlinear control. Thanks to its well-known characteristics of robustness, high-speed response, insensitivity to the variable parameters and easy implementation [17, 18], this control technique has been widely used in the non-linear system [19–21]. However, in spite of the advantages that can provide a SMC, its implementation may be obstructed by an undesirable harmful phenomenon, which is known as 'chattering'. In the aim to alleviate this drawback, numerous techniques have been proposed in the literature [22, 23].

The present paper proposes a control design of wind turbine-PMSG system aimed to low electrical power supply in isolated sites. The configuration of the overall system is illustrated in Fig. 1, where the PMSG is connected to the wind turbine directly. The PMSG generates electrical power and supplies the load through a PWM rectifier via a dc link. The goal of the control system is mainly to keep the dc voltage constant regardless of wind speed profile and supply loads variations. For this, sliding mode control algorithm is proposed. Three SMCs in all composed the control system; one in the external loop to control the dc-voltage, and two other in the internal loops to ensure the current control and tracking. The control strategy takes a cascaded structure; the external dc voltage-SMC generates the reference of the quadratic current component. Therefore, it depends on the discontinuous control of the outer controller which implies that this reference will have a discontinuous behavior. Hence, the waveforms of the currents are completely distorted. To overcome this problem, we will introduce an hyperbolic tangent function instead of conventionally used sign function. So, the transient of the hitting control will be smoothed without losing the system robustness.

To ensure the reaching and sustaining of the sliding mode, we use the Lyapunov direct method. The space vector modulation (SVM) technique is used to calculate the logic control signals (S_a, S_b, S_c). The SVM technique improves the current-steady state performance by reducing harmonics. This will allow the control system to operate with a fixed switching frequency. Finally, the simulation results, performed under Matlab / Simulink, are presented and analyzed. They confirm that the proposed control system provides high dynamic characteristics and very strong robustness to external load disturbances.

2. WIND ENERGY CONVERSION SYSTEM DESCRIPTION

2.1. WIND TURBINE MODEL

The aerodynamic power is given as [24]:

$$P_T = 0.5A\rho C_p(\lambda)v_w^3, \tag{1}$$

where A is the blade swept area, ρ is the air density, v_w is the wind speed.

The turbine power coefficient $C_p(\lambda)$ is expressed by the following equation (2).

$$C_p(\lambda) = -0.2121\lambda^3 + 0.0859\lambda^2 + 0.2539\lambda. \tag{2}$$

The tip-speed ratio λ is a relation of shaft speed (ω_m) and the wind speed, as follow:

$$\lambda = \frac{R\omega_m}{v_w}, \tag{3}$$

where R is the radius of the wind turbine.

The mechanical torque is given by:

$$T_T = 0.5\rho A\frac{C_p(\lambda)}{\omega_m}v_w{}^3 . \tag{4}$$

The motion equation can be expressed by equation (5):

$$T_T = J\frac{d\omega_m}{dt} + F\omega_m + T_e, \tag{5}$$

where T_T is the turbine torque, J is the total equivalent inertia of turbine and PMSG, F is the damping coefficient, and T_e is the electromagnetic torque of the generator.

2.2. PMSG MATHEMATIC MODEL

PMSG model is given compared to its equivalent circuit, expressed in the synchronous dq coordinates, as follow [25]:

$$v_q = -R_s i_q - L_s\frac{di_q}{dt} - \omega L_s i_d + \omega\psi \quad , \tag{6}$$

$$v_d = -R_s i_d - L_s\frac{di_d}{dt} + \omega L_s i_q \quad , \tag{7}$$

where R_s is the resistance of stator winding, v_d, v_q, i_d and i_q are the dq components of stator voltage and current, respectively, L_s the stator winding inductance, ψ is the magnetic flux and ω is he generator electrical angular speed. The generator electromagnetic torque is given by the following expression:

$$T_e = \frac{3}{2}p\psi i_q, \tag{8}$$

where p is the pole pair number.

2.3. PWM RECTIFIER MODEL

The dynamic model of PWM rectifier in synchronous rotating dq reference frame is expressed by equations (9–11) [26]:

$$v_q = R.i_q + L\frac{\mathrm{d}i_q}{\mathrm{d}t} + L.\omega i_d + v_{rq} \ , \tag{9}$$

$$v_d = R.i_d + L\frac{\mathrm{d}i_d}{\mathrm{d}t} - L.\omega i_q + v_{rd} \ , \tag{10}$$

$$C\frac{\mathrm{d}V_{dc}}{\mathrm{d}t} = i_{dc} - i_L = \frac{3}{2}(S_d i_d + S_q i_q) - \frac{V_{dc}}{R_L} \ . \tag{11}$$

3. DESIGN CONTROLLER

The control goal is to keep the dc-voltage constant at its reference value. For this purpose, the sliding mode control technique is used. SMC is a robust nonlinear algorithm, it uses a discontinuous control in the goal is to force the system trajectories to join a specified slip surface. The transient dynamic response of the system is dependent on the choice of the sliding surface, which is not unique [27].

In the case of this paper, three sliding surfaces related to control objectives are defined, as follow:

$$S(i_q) = i_q^{\,*} - i_q \ , \tag{12}$$

$$S(i_d) = i_d^{\,*} - i_d \ , \tag{13}$$

$$S(V_{dc}) = V_{dc}^{\,*} - V_{dc} \ . \tag{14}$$

The sufficiency conditions for the existence and sustaining of the sliding mode is given as follow [27]:

$$S(x)\dot{S}(x) \le -\eta|S| \ . \tag{15}$$

A commonly used form of the control law is:

$$U = -K_x \mathrm{sign}(S(x)), \tag{16}$$

where K_x is the gain of the SMC, and:

$$\mathrm{sign}(S(x)) = \begin{cases} +1 & \text{if} \quad S(x) > 0 \\ 0 & \text{if} \quad S(x) = 0 \\ -1 & \text{if} \quad S(x) < 0 \end{cases} . \tag{17}$$

In the following, we will design the corresponding control law for each sliding surface.

3.1. CURRENT CONTROL DESIGN (*dq* axes)

The q and d axes current state variables are given as follow:

$$\frac{\mathrm{d}i_q}{\mathrm{d}t} = \frac{1}{L}v_q - \frac{R}{L}i_q - \omega.i_d - \frac{1}{L}v_{rq} \ , \tag{18}$$

$$\frac{\mathrm{d}i_d}{\mathrm{d}t} = \frac{1}{L}v_d - \frac{R}{L}i_d + \omega.i_q - \frac{1}{L}v_{rd} \ . \tag{19}$$

Differentiating (12) with respect to time and substituting corresponding relation from (18) yields:

$$\dot{S}(i_q) = \frac{\mathrm{d}i_q^{\,*}}{\mathrm{d}t} - \left(\frac{1}{L}v_q - \frac{R}{L}i_q - \omega.i_d\right) + \frac{1}{L}v_{rq} . \tag{20}$$

Substituting (20) into (15) and using (16) the sliding mode control law of the q axis current component is obtained as:

$$v_{rq}^{\,*} = -K_q \mathrm{sign}(S(i_q)) + \left(v_q - R.i_q - \omega L i_d - L\frac{\mathrm{d}i_q^{\,*}}{\mathrm{d}t}\right). \tag{21}$$

By repeating exactly the same procedure for the d-axis current component, we obtain the following control law:

$$v_{rd}^{\,*} = -K_d \mathrm{sign}(S(i_d)) + \left(v_d - R.i_d + \omega L i_q - L\frac{\mathrm{d}i_d^{\,*}}{\mathrm{d}t}\right). \tag{22}$$

As it can be seen in (21) and (22), there are two terms in the control law, continuous and discontinuous. The continuous term reflects knowledge of the system dynamics. The discontinuous one ensures the sliding to occur. However, this controller leads to limited performance due to the high control activity resulting in chattering. To reduce the latter, a boundary layer method substitutes the discontinuity of a SMC by a saturation function, which results in a smooth control signal [28].

Then, the control laws (21) and (22) become:

$$v_{rq}^{\,*} = -K_q \,\mathrm{sat}\left(\frac{S_q}{\text{Ø}}\right) + \left(v_q - R i_q - \omega L i_d - L\frac{\mathrm{d}i_q^{\,*}}{\mathrm{d}t}\right), \tag{23}$$

$$v_{rd}^{\,*} = -K_d \,\mathrm{sat}\left(\frac{S_d}{\text{Ø}}\right) + \left(v_d - R.i_d + \omega L i_q - L\frac{\mathrm{d}i_d^{\,*}}{\mathrm{d}t}\right), \tag{24}$$

where

$$\mathrm{sat}\left(\frac{S}{\text{Ø}}\right) = \begin{cases} \dfrac{S}{\text{Ø}} & \text{if} \quad |S| \le \text{Ø} \\ \mathrm{sign}(S) & \text{if} \quad |S| > \text{Ø} \end{cases} \tag{25}$$

And Ø represent the bandwidth of the saturation function.

3.2. DC-VOLTAGE CONTROL DESIGN

The dc-voltage state equation is given as follow:

$$\frac{\mathrm{d}V_{dc}}{\mathrm{d}t} = -\frac{i_L}{C} + \frac{i_{dc}}{C} = -\frac{V_{dc}}{R_L.C} + \frac{i_{dc}}{C}. \tag{26}$$

In similar manner as in previous section, the sliding mode control law of the dc voltage is described as follow:

$$i_{dc}^{\,*} = K_{dc}\mathrm{sign}(S(V_{dc})) + \frac{V_{dc}}{R_L}. \tag{27}$$

Multiplying (27) by V_{dc}, then the reference output power is obtained:

$$P_{dc}^{\,*} = V_{dc}.i_{dc}^{\,*}. \tag{28}$$

By neglecting the converter losses and assuming that $i_d = 0$, we can write:

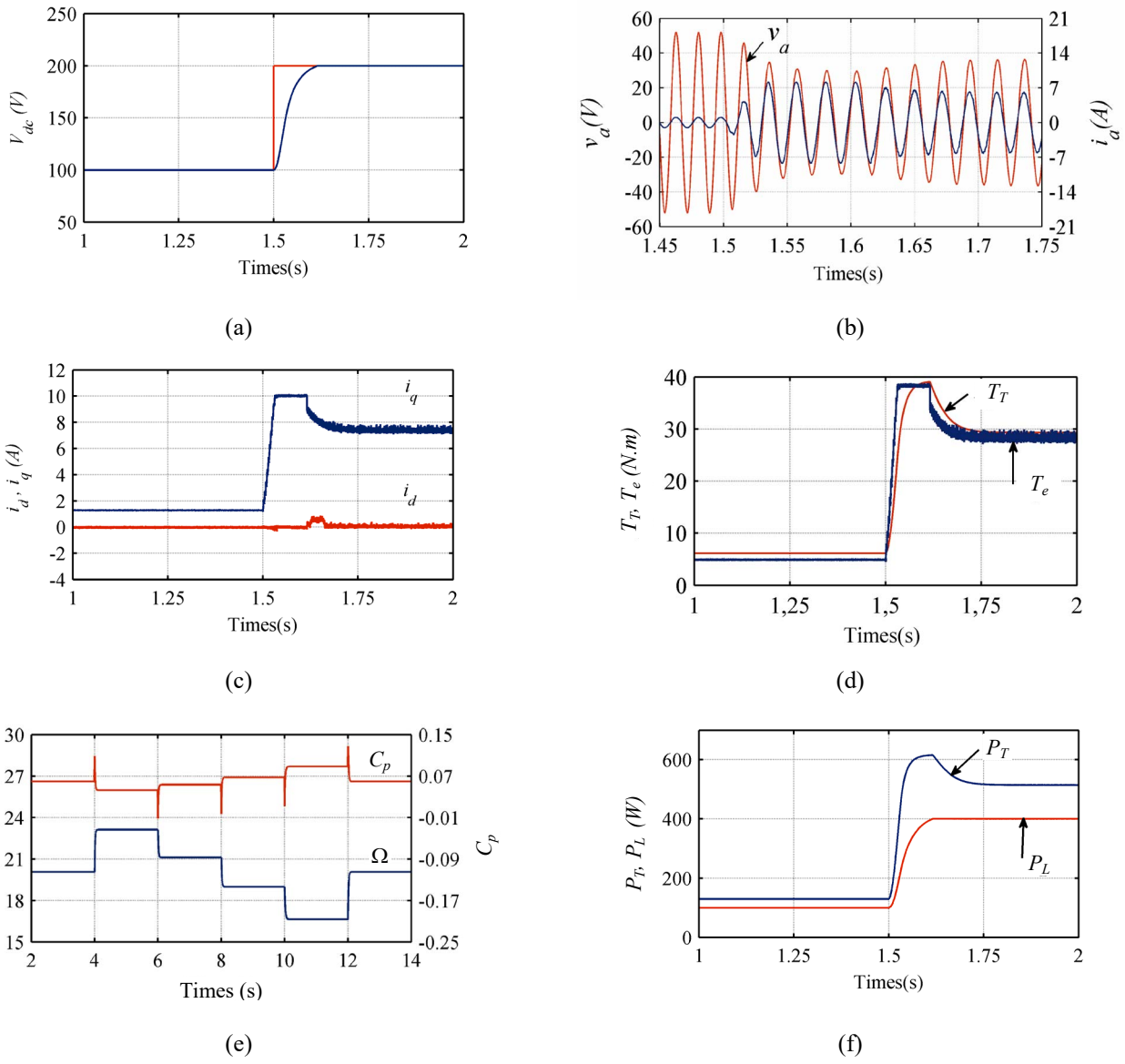

Fig. 2 – Simulation results for a step change in V_{dc}: a) V_{dc}, b) v_a and i_a, c) i_d and i_q, d) T_T and T_e, e) Ω and C_p, f) P_T and P_L.

$$P_{dc} = V_{dc}.i_{dc} = v_q.i_q \,. \tag{29}$$

Therefore, the q- current reference is given by:

$$i_q^{\,*} = \frac{V_{dc}}{v_q}\left(K_{dc}\,\mathrm{sign}(S(V_{dc})) + \frac{V_{dc}}{R_L}\right). \tag{30}$$

Note that, because the reference of the q axis current component is generated by a SMC which have a discontinuous control action, causes ripples to the ac side currents (chattering phenomenon), this reference switch from a given maximal value to a minimal value. Hence, the waveforms of the ac side currents are affected and are much distorted. To alleviate the chattering phenomenon, we will introduce an hyperbolic tangent function instead of sign function. So, the transient of the hitting control will be smoothed. Therefore, the equation (31) becomes:

$$i_q^{\,*} = \frac{V_{dc}}{v_q}\left(K_{dc}\tanh\left(\frac{S(V_{dc})}{\varepsilon}\right) + \frac{V_{dc}}{R_L}\right), \tag{31}$$

where ε defines the thickness of the boundary layer.

4. SIMULATION RESULTS

The model of the PMSG based WECS of Fig. 1 is built using Matlab/Simulink. The parameters of the overall system are given in Table I. The switching frequency used for the simulation is 10^4 Hz.

To evaluate the dynamic performance of the control scheme, a step change in dc link voltage (100 to 200 V at t = 1.5 s) is applied under resistive load (R_L = 100 Ω) and constant wind speed (v_w = 12.5 m/s). The simulation results are shown in Fig.2.a–f. It can be seen from Fig. 2.a, that the system exhibits high dynamic characteristics. Waves of phase voltage and phase current are shown in Fig.2.b. We can see that input current is close to sine wave and has the same phase in respect with phase voltage. Figure 2.c displays the d and q components of stator current, which shows that the d component is set to zero and the q component takes a non-null value to produce generator torque. Figure 2.d represents generator and wind turbine torque. Figure 2.e illustrates the evolution of generator speed and power coefficient while in Fig. 2.f is displayed the plots of load and turbine power. As can be observed, when the dc link voltage steps up from 100 to 200 V, the

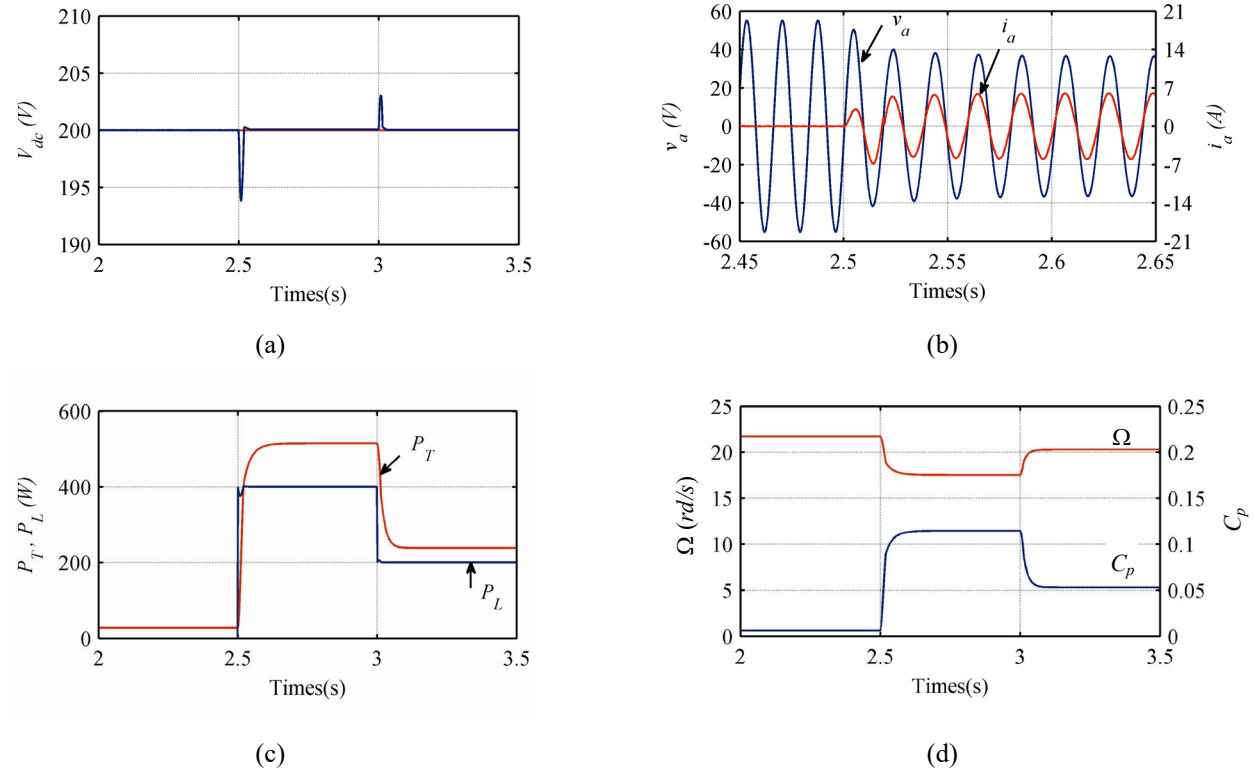

Fig. 3 – Simulation results for load changes: a) V_{dc}, b) v_a and i_a, c) P_T and P_L, d) Ω and C_p.

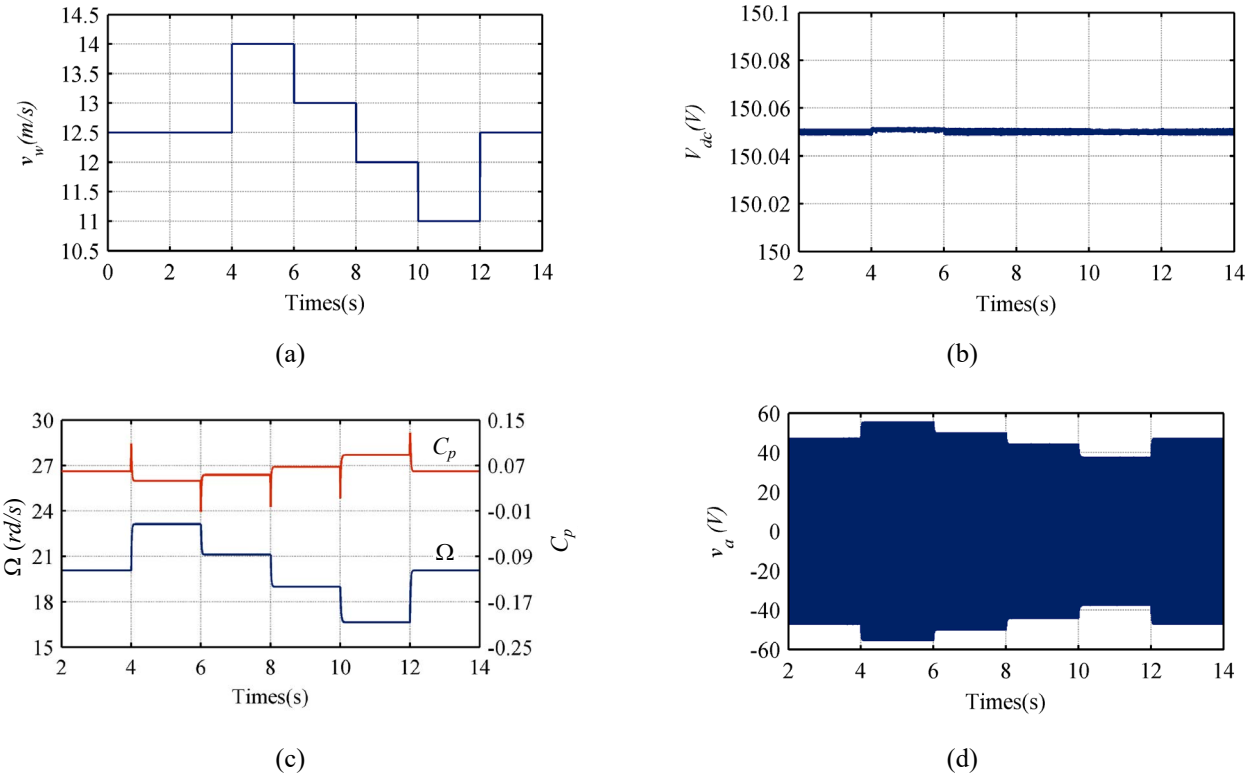

Fig. 4 – Simulation results for speed wind changes: a) v_w, b) V_{dc}, c) Ω and C_p, d) v_a.

load demand increase from 100 to 400 W, what causes increasing of power coefficient and decreasing of generator speed. It is significant to note that the power generated by wind turbine is greater than the load demand power to compensate losses by frictions ($F.\omega_m^2$) and losses in the generator stator windings ($1.5\ R_s.I_q^2$).

The effect of load variations on the operation of the system is illustrated by Fig. 3.a–d. In this test, the wind velocity considered is v_w= 12.5 m/s and the dc voltage value is fixed to 200 V. Initially unloaded, the system operates from t = 2.5 s with 100 Ω resistive load and at t = 3 s, the load value is changed to 200 Ω. As it is shown in Fig.3.a, load variations has very limited effects on the dc voltage which remains almost constant. Figure 3.b shows that phase current value initially near to zero takes at time instant (t = 2.5 s) where load is applied a nonnull value to

satisfy load power demand expressed by the plot shown in Fig. 3.c. Figure 3.d shows the evolution of generator speed and power coefficient.

Figures 4.a–d show simulation results obtained with variable wind speed profile (Fig.4.a). As can be observed in Fig. 4.b, the dc link voltage is clearly no sensitive to wind variations. Fig.4.c and d show plots of generator speed, power coefficient and phase voltage.

5. CONCLUSION

In this study, a sliding mode control of a PMSG driven wind energy conversion system is presented. Regarding the simulation results, we can obtain the following conclusions:

– The control algorithm studied in this work exhibits high dynamic characteristics.

– The proposed control scheme is robust against load changes and is no sensitive to wind speed variations.

– In addition, the sliding mode control system has some advantages in terms of few tuned parameters, Simple structure and easy implementation comparatively with classical PI controller.

APPENDIX

The parameters of the whole system are given in the Table 1.

Table 1
System parameters

PMSG AND WIND TURBINE PARAMETERS				RECTIFIER PARAMETERS	
Parameter	Value	Parameter	Value	Parameter	Value
V_n	90 V	Φ_{eff}	0.15 Wb	R	0.1 Ω
I_n	4.8 A	A	3.75 m^2	L	0.01 H
P_n	600 W	ρ	1.2 kg/m^3	C	1000 mF
R_s	1.137 Ω	J	0.1 kg.m^2		
L_s	2.7 mH	B	0.06 N.m.s/rad		

Received October 31, 2018

REFERENCES

1. S. Nikolova, A. Causevski, A. Al-Salaymeh, *Optimal operation of conventional power plants in power system with integrated renewable energy sources*, Energy Convers. Manage., **65**, pp. 697–703 (2013).
2. R. Mittal, K.S. Sandu, D.K. Jain, *Isolated operation of variable speed driven PMSG for wind Energy conversion system*, Int. J. Eng. Technol. (IACSIT), **1,** *3*, pp. 269–273 (2009).
3. H. Li, K.L. Shi, P. McLaren, *Neural network based sensorless maximum wind energy capture with compensated power coefficient*, IEEE Trans. Ind. Appl., **41**, *6*, pp. 548–1556 (2005).
4. R. Ahshan, M.T. Iqbal, G.K.I. Mann, *Controller for a small induction-generator based wind-turbine*, Appl Energy., **85**, *4*, pp. 218–227 (2008).
5. T. Ackermann: *Wind power in power systems,* England, Wiley (2005).
6. J.A. Baroudi, V. Dinavahi, A.M. Knight, A review of power converter topologies for wind generators, Renew. Energy., **32**, pp. 2369–2385 (2007).
7. M.E. Haque, K.M. Muttaqi, M. Negnevitsky, *A novel control strategy for a variable speed wind turbine with a permanent magnet synchronous generator*, IEEE Trans. Ind. Appl., **46**, *1*, pp. 331–339 (2010).
8. J. Dai, D. Xu, B. Wu, *A novel control scheme for current-source converter-based PMSG wind energy conversion systems*, IEEE Trans. Power Electron., **24**, *4*, pp. 1–10 (2009).
9. X. Yuan, F. Wang, R. Burgos, Y. Li, D. Boroyevich, *Dc-link voltage control of full power converter for wind generator operating in weak grid systems*, Proceedings of 23th Annual Conference of IEEE Applied Power Electronics, pp. 761–767 (2008).
10. A. Dahbi, M. Hachemi, N. Nait-Said, M.S. Nait-Said, *Realization and control of a wind turbine connected to the grid by using PMSG*, Energy Convers. and Manage., **84**, pp. 346–353 (2014).
11. C.M. Hong, C.H. Chen, C.S. Tu, *Maximum power point tracking-based control algorithm for PMSG wind generation system without mechanical sensors*, Energy Convers. Manage., **69**, pp. 58–67 (2013).
12. J.; Belhadj, X. Roboam, *Investigation of different methods to control a small variable-speed wind turbine with PMSM drives*, J. Energy Resour. Technol., **129**, *3*, pp. 200–213 (2006).
13. M. Chinchilla, S. Arnaltes, J.C. Burgos, *Control of permanent-magnet generators applied to variable-speed wind-energy systems connected to the grid*, IEEE Trans. Energy Convers., **21**, *1*, pp. 130–135 (2006).
14. A.Z. Mohamed, M.N. Eskander, F.A. Ghali, *Fuzzy logic control based maximum power tracking of a wind energy system*, Renew. Energy, **23**, *2*, pp. 235–245 (2001).
15. M. Pahlevaninezhad, S. Eren, A. Bakhshai, P. Jain, *Maximum power point tracking of a wind energy conversion system using adaptive nonlinear approach,* Twenty-Fifth Annual IEEE Applied Power Electronics Conference and Exposition (APEC), pp. 149–154 (2010).
16. W. Qiao, L. Qu, R. Harley, *Control of ipm synchronous generator for maximum wind power generation considering magnetic saturation,* IEEE Industry Applications Conference. 42nd IAS Annual Meeting, pp. 1265–1272 (2007).
17. A. Boucheta, I. K. Bousserhane, A. Hazzab, B. Mazari, M. K. Fellah, *Fuzzy sliding mode controller for linear induction motor control,* Rev. Roum. Sci. Techn. – Électrotechn. et Énerg., **54**, *4*, pp. 405–414 (2009).
18. A. Ahriche, M. Kidouche, A. Idir, Y. Deia, *Combining sliding mode and second Lyapunov function for flux estimation*, Rev. Roum. Sci. Techn. – Électrotechn. et Énerg., **61**, *2,* pp. 106–110 (2016).
19. T.L. Chern, Y.C. Wu, *Integral variable structure control approach for robot manipulators,* IEE Proceeding of Control Theory and Applications **139**, *2*, pp. 161–166 (1992).
20. A. Aberbour, K. Idjdarene, Z. Boudries, *Adaptable sliding mode control for wind energy application,* Rev. Roum. Sci. Techn. – Électrotechn. et Énerg., **61**, *3,* pp. 258–262 (2016).
21. Y. Deia, M. Kidouche, M. Becherif, *Decentralized robust sliding mode control for a class of interconnected nonlinear systems with strong interconnections,* Rev. Roum. Sci. Techn. – Électrotechn. et Énerg., **62**, *2,* pp. 203–208 (2017).
22. L.K. Wong, F.H.F. Leung, P.K.S. Tam, *A chattering elimination algorithm for sliding mode control of uncertain non-linear systems*, Mechatronics Elsevier Science, **8**, *7*, 765–775 (1998).
23. F.J. Chang, S.H. Twu, S. Chang, *Adaptive chattering alleviation of variable structure systems control*. IEE Proceedings D of Control Theory and Applications, **137**, *1*, pp. 31–39 (1990).
24. S. Arezki, M. Boudour, *Study and regulation of dc bus voltages of wind-photovoltaic system*, Rev. Roum. Sci. Techn. – Électrotechn. et Énerg., **59**, *1,* pp. 35–46 (2014).
25. M. Chinchilla, S. Arnalte, J.C. Burgos, *Control of permanent-magnet generators applied to variable-speed wind-energy systems connected to the grid*, IEEE Trans. Energy convers, **21**, *1*, pp. 130–135 (2006).
26. Z. Boudries, A. Aberbour, K. Idjdarene, *Study on sliding mode virtual flux oriented control for three-phase PWM rectifiers,* Rev. Roum. Sci. Techn. – Électrotechn. et Énerg., **61**, 2 , pp. 153–158 (2016).
27. V.I. Utkin, *Variable structure systems with sliding modes – a survey*, IEEE Trans. Autom. Control, **22**, *2*, pp. 212–222 (1997).
28. M.W. Dunnigan, S. Wade, B.W. Williams, X. Yu, *Position control of a vector controlled induction machine using Slotine's sliding mode control approach.* IEE Proceedings of Electric Power Applications **145**, *3*, pp. 231–238 (1998).